DOE/ET-53088-270 IFSR #270

Two-Dimensional Shear Flow Turbulence: A Statistical Theory of Vortex Filaments

Tzihong Chiueh

Department of Astrophysical, Planetary,
and Atmospheric Sciences
The University of Colorado
Boulder, Colorado 80309

P. W. Terry and *P. H. Diamond*

Institute for Fusion Studies
The University of Texas at Austin
Austin, Texas 78712

May 1987

Two-Dimensional Shear Flow Turbulence: A Statistical Theory of Vortex Filaments

Tzihong Chiueh
Department of Astrophysical, Planetary,
and Atmospheric Sciences
The University of Colorado
Boulder, Colorado 80309

and

P. W. Terry and *P. H. Diamond*
Institute for Fusion Studies
The University of Texas at Austin
Austin, Texas 78712

Abstract

A theory of two-dimensional free shear flow turbulence is proposed. In particular, the role of interactions of fluctuations with the mean flow is distinguished from that of interactions among fluctuations. The former are responsible for the extraction of free energy necessary for maintaining the turbulence, while the latter lead to the enstrophy cascade which generates small-scale eddies. On the length scales of greatest interest, turbulence is anisotropic because of the influence of mean flow shear. At smaller scales, self-similar enstrophy transfer occurs and yields the familiar power law spectrum. Free energy extraction is accompanied by mean flow relaxation. Two distinct mechanisms are involved. In addition to the usual quasilinear diffusion, there is a nonlinear drift which acts to enhance localized fluctuations and flatten the mean flow profile. The saturated state is characterized by collective resonances which must be nonlinearly damped in order to balance their generation by seed-eddy induction. This balance gives rise to a condition for the determination of the nonlinear damping rate, and thus the turbulence level. The spatial structure of the saturated fluctuations is also predicted.

I. Introduction

The role of eddies in fluid turbulence has been emphasized in the past few decades. Early studies by Taylor,[1] Prandtl,[2] Von Karman,[3] and others developed the concept of a mixing length, in which eddies are treated as individual quasi-particles obeying the laws of kinetic theory. Later, Kolmogoroff[4] and Obukhov[5] extended this concept by incorporating a cascade of energy from large eddies to small ones. More recently, Novikov,[6] Nelkin,[7] Mandelbrot,[8] Frisch et al.,[9] and Mori[10] have refined these ideas in an attempt to explain intermittency in fluid turbulence.

In these studies, homogeneous and isotropic turbulence is usually assumed. This is based on the presumption that when the eddies of interest are sufficiently small, they do not sense the inhomogeneity of the system and are thus isotropic. Such an argument is valid for 3-D turbulence, but not for 2-D shear flow turbulence. The reason is that 3-D eddies "turn over" faster as their sizes decrease, a consequence of vortex stretching and the conservation of angular momentum of spinning flux tubes. Consequently, variation of the large scale appears adiabatic, and doesn't affect the small-scale eddies. By contrast, 2-D eddies of different sizes turn over at nearly the same rate.[11] Thus, large-scale motion can easily influence the small eddy dynamics. In particular, small eddies may be sheared apart by the large-scale motion. The shearing thus contributes to the determination of the eddy turnover time. Indeed, this phenomenon has led to consideration of a nonlocal cascade of enstrophy in 2-D turbulence.[11]

It is also clear that the basic dynamics of 2-D isotropic and homogeneous turbulence are quite different from that of 2-D shear flow turbulence, in several respects. These differences can be best illustrated by a comparison of relevant time scales. For isotropic and homogeneous turbulence, nonlinear stresses control the dynamics of virtually all interesting scales. In the inertial range, the time scale of relevance is the nonlinear scrambling time, τ_c, which measures the lifetime of an eddy before it is sheared apart. By contrast, shear flow turbulence has an additional time scale due to the existence of a sheared mean flow. In the linear limit, the existence of this scale underlies the Rapid Distortion Theory[12] of Townsend. This time scale is associated with the lifetime of excited waves (Tolmien-Schlicting waves in the viscous case) which originate as a consequence of the mean shear

flow. Wave lifetime is gauged by the frequency spectrum linewidth $\Delta\omega_k$. In shear flows, the spectrum width and the scrambling rate can be estimated respectively to be $\Delta V_0/\Delta L_0$ and $\epsilon\Delta V_0/\Delta L_0$, where ΔV_0 and ΔL_0 are the characteristic speed and size of the flows. The scrambling rate $\epsilon\Delta V_0/L_0$ is obtained from a mixing-length estimate and is proportional to the growth rate of linear instability. The ratio of these two times, ϵ^{-1}, is usually much larger than unity, except for mixing layer flows, which shall be excluded from our study. As a consequence, collective resonances, which satisfy a dispersion relation and do not otherwise occur in the isotropic and homogeneous case, seem to play a significant role in 2-D shear flow turbulence. In most previous work describing inhomogeneous turbulence, linearization of the equations and dispersion relations are the primary focii.[13] Typically wave–wave coupling analyses[14] (weak turbulence theory) or Landau-Ginzburg type amplitude equations[13] have been used for the description of evolution of linearly unstable modes. There are also studies[15,16] of the dynamics of a few eddies in an inviscid fluid. These studies are the dynamical counterparts of the statistical approach to be developed in this work.

In most realistic situations, systems are weakly dissipative. Fluctuation spectra are broad-band, and cannot be described by a few modes or solely by dispersion relations. Along with large-scale wave fluctuations, there also exist small-scale localized fluctuations, commonly referred to as eddies.[12] Eddies do not obey dispersion relations and are locally convected by the mean flows. In Fourier representation, their components obey $\omega = kV_0$, where ω, k, V_0 are the frequency, wavevector, and mean flow velocity, respectively. In linear analysis of 2-D shear flows these "ballistic" modes exist, but are usually ignored since they are damped, albeit weakly. They correspond to local resonances with the mean flow. Near the resonant points, nonlinearity can strongly modify the resonance.[18] Indeed, the stream function ϕ in the resonance layer forms "island" chains, conventionally called "Kelvin's cat's eyes." The cat's eyes appear when the nonlinearity exceeds viscosity, that is, when the viscous layer width ℓ_ν is much smaller than the nonlinear layer width $\ell_{\rm NL}$, where $\ell_\nu \sim \nu^{1/3}$, ν is viscosity, $\ell_{\rm NL} \sim \phi^{1/2}$, and ϕ is the perturbation amplitude. In such a regime, the viscous layer is confined to the cat's-eye separatrices. It has been shown in a numerical calculation[19] of nonlinear critical layers that starting with an initially

smooth distribution, vorticity quickly builds up and concentrates near the separatrices. The concentrated vorticity appears to consist of paired vortex strips of opposite signs at the upper and lower branches of the separatrices. In fully developed turbulence, cat's eyes overlap so that the vortex pairs must break up, and the individual vortex filaments of opposite signs thus constitute the eddies in 2-D shear flow turbulence.

Since 2-D turbulence contains both waves and eddies of the kind mentioned above, the presence of one component must affect the dynamics of the other. Their relationship can be viewed as follows. In stationary, fully developed turbulence, waves must be damped, and thus support a finite resonance width. Indeed, wave-like fluctuations can be induced by seed eddies, but can last only for a wave damping time due to exchange of angular momentum with the eddies that are trapped by waves. (Filamentary vortices[20] are entrained into the cat's eyes by the roll-up motion of waves.) As a result of angular momentum exchange, eddies are scattered and sheared apart into smaller ones. This is precisely the process leading to enstrophy cascade in 2-D turbulence. More importantly, eddies of sufficiently large size can extract free energy from the mean flow rapidly, allowing eddy-wave interaction to continue. This is the picture of fully developed 2-D turbulence proposed here. Hence, this work is motivated by the contention that the previous phenomenological models of eddy cascade in shear flow turbulence did not account for realistic driving sources associated with flow inhomogeneities and that the nonlinear wave theories fail to incorporate an important constituent of turbulence, i.e., eddies which are not eigenmodes.

The theory to be developed in this work has been previously explored by Dupree.[23] Dupree has studied homogeneous and isotropic 2-D turbulence, and shown that the enstrophy cascade can be viewed as imperfect turbulent mixing, where turbulent scrambling cannot efficiently resolve structures smaller than the average scale of the turbulence. (This had actually been pointed out previously by Kraichnan.[11]) In shear flows, the static mean flow shear can combine with straining to accelerate the eddy turnover rate. This follows from the fact that, as pointed out earlier, the vortices become filaments elongated along the mean flow. Thus, they can precess about their minor axes at a rate which can be much faster than turnover in the absence of mean flow. As a consequence of the mean flow shear, the turbulence spectrum now becomes anisotropic, reflecting the presence of filamentary

vortex structures. We will show that the mean flow shear only affects the contour shape of the k-spectrum but not the dependence on k. This implies that in saturated turbulence the energy exchange between the mean flow and fluctuations is limited to large scales. At smaller scales, the mean flow does not directly interact with the eddies, and thus the energy spectrum of small fluctuations is unchanged.

Two distinct mechanisms are responsible for free energy extraction, and follow from the relationship between the generation of the fluctuations and mean flow relaxation. The conservation law of vorticity for two-dimensional inviscid motion of a fluid element, $\partial\rho/\partial t = 0$, relates the dynamics of vorticity fluctuations $\delta\rho$ relaxation of the mean flow vorticity $\langle\rho\rangle$ through the relation

$$\frac{\partial}{\partial t}\int \langle\delta\rho^2\rangle\, dx = -\frac{\partial}{\partial t}\int \langle\rho\rangle^2\, dx, \tag{2}$$

where $\rho = \nabla^2\phi$ is the vorticity.

This equation shows that fluctuation growth is ultimately related to the mean vorticity decay. The two mechanisms of energy extraction follow from this relation and are (a) turbulent rearrangement of vortex elements, and (b) nonlinear drift of eddies along the mean vorticity gradient. Turbulent mixing brings together fluid elements of different vorticity (originally located at very different positions along the mean vorticity gradient), and thus enhances the local vorticity gradient. The nonlinear drift arises because individual eddies induce a velocity field that scatters the eddy down or up the mean vorticity gradient, according to the sign of the fluctuation relative to the local mean value. The direction of the drift is such that a positive fluctuation moves up the gradient, and a negative one down the gradient. The net result of these two processes is the flattening of the mean vorticity slope, and the expansion of the mean flow. The situation where the mean vorticity decreases and the mean flow broadens is consistent with a scenario of enstrophy cascade[11] in 2-D flows.

Throughout this work, we shall assume a separation of time scales. There are three time scales involved in this problem. The fastest time scale is that of the mean flow shear or the mean flow convection, and the typical value is L_0/V_0, where L_0 and V_0 are characteristic length and velocity, respectively. The next time scale is the eddy turnover

time, which will be shown to be approximately the nonlinear scrambling time multiplied by a factor $\ln(L_0/\Delta X)$, where ΔX is the eddy size. This ΔX dependence arises from the fact that the shearing time is longer for small eddies than it is for large ones. The slowest time scale is the mean flow relaxation time. Of course, this may not be true in the early stage of a linearly unstable flow, where the mean flow loses energy rapidly. However, after unstable wave fluctuations are saturated, the mean flow evolution slows dramatically and a quasi-stationary state is achieved. This has been observed in experiments.[24]

In this paper, we shall be content with an analytical treatment of two-dimensional, rather than three-dimensional, turbulence, for reasons of its simplicity. Nevertheless, two-dimensional flows actually occur in many real circumstances. For example, a strongly magnetized plasma ($\beta \ll 1$) can be well described by the 2-D Navier-Stoke equation,[24,25] or the Hasegawa-Mima equation[26] (a slight variation of the N-S equation taking into account electron motion along field lines). Large-scale atmospheric motion, such as Rossby waves[27] driven by the earth's rotation, can also be well approximated by a 2-D flow. Phenomena in astrophysical environments, such as thin accretion disks, can also be treated with two-dimensional models.[28] Another interesting realization of 2-D flows is the X-Y model of lattice gas in condensed matter physics.[29] Here, two-dimensional geometry is easily realized in a lattice, and the topological defects of spin angles can be identified as point vortices, whose dynamics obeys the Euler's equations of two-dimensional fluids. Conventional studies in this area usually concentrate on the onset of turbulence, where critical phenomena occur. In the stage of fully developed turbulence, studies of fluids may prove to be of great use in this field.

The organization of this paper is as follows: in Sec. II we examine some basic conservation laws of 2-D flows in the inviscid limit. The importance of these conservation laws will become apparent in the subsequent section (Sec. III), where triplet nonlinearities in the two-point vorticity equation are modeled by relative turbulent diffusion. In Sec. III we consider the evolution of flows on the slow, nonlinear time scale where the evolution is best described by the two-point vorticity correlation equation. We also show that in shear flow turbulence, small eddies are torn apart at a rate much faster than in homogeneous turbulence. In Sec. IV we focus on the driving source of fluctuations. The two mecha-

nisms for free energy extraction, the rearrangement and the drift of eddies, are discussed. In Sec. V we solve the two-point vorticity correlation equation for stationary turbulence, and obtain the vorticity k-spectrum. Basically, the two-point equation describes a competition between turbulent decorrelation and generation of eddies. Balance of the two competing processes imposes a condition for stationary turbulence. It is this condition that ultimately determines the fluctuation level and the average eddy size. Physically, this means that turbulence is regulated by fluctuation amplitudes and the eddy size in order to maintain stationarity. Finally, we discuss applications and future extensions of this work in Sec. VI.

II. Basic Equations and Conservation Laws

The turbulent velocity field $\mathbf{V}$ obeys the Navier-Stokes equation

$$\left(\frac{\partial}{\partial t}+\mathbf{V}\cdot\nabla\right)\mathbf{V}=-\frac{1}{m}\nabla(P+\psi)+\nu\nabla^2\mathbf{V} \tag{3}$$

where m, P, ψ, and ∇^2 are the mass density, pressure, external force potential, and two-dimensional Laplacian. The Navier-Stokes equation can equivalently be expressed as an evolution equation for vorticity ρ

$$\left(\frac{\partial}{\partial t}+\mathbf{V}\cdot\nabla\right)\rho=\nu\nabla^2\rho, \tag{4}$$

where $\rho=\partial V_y/\partial x-\partial V_x/\partial y=\nabla^2\phi$, and ϕ is the stream function for a 2-D incompressible velocity field $\mathbf{V}=\hat{y}(\partial\phi/\partial x)-\hat{x}(\partial\phi/\partial y)$.

In the limit of vanishing viscosity, Eq. (4) describes conservation of vorticity in an infinitesimal fluid element. Vorticity is convected by the fluid element to which it was initially assigned. The convection of vorticity by the flow is similar to the convection of a passive scalar such as dye or markers, with one crucial difference. Vorticity can feedback and influence velocity fields through the relation

$$\phi(\mathbf{x})=\cdot\int d\mathbf{x}'\nabla^{-2}(\mathbf{x},\mathbf{x}')\rho(\mathbf{x}'), \tag{5}$$

where $\nabla^{-2}(\mathbf{x},\mathbf{x}')$ is the inverse Laplacian. This is simply the Biot-Savart law. The squared vorticity obeys a global conservation law

$$\frac{\partial}{\partial t}\int d\mathbf{x}\rho^2(\mathbf{x})=-\nu\int d\mathbf{x}\left(\nabla\rho(\mathbf{x})\right)^2. \tag{6}$$

In addition, the product of vorticity ρ and the stream function ϕ obeys another conservation law. After integration by parts, this conservation law represents conservation of fluid kinetic energy

$$\frac{\partial}{\partial t}\int d\mathbf{x}(\nabla\phi)^2 = -\nu\int d\mathbf{x}\rho^2. \tag{7}$$

(The condition of incompressibility eliminates the fluid internal energy.) Both enstrophy and kinetic energy are conserved up to viscous dissipation. The triplet nonlinearities, $\int d\mathbf{x}(\rho\mathbf{v}\cdot\nabla\rho)$, and $\int d\mathbf{x}\,(\mathbf{v}\cdot(\mathbf{v}\cdot\nabla\mathbf{v}))$, do not contribute to the global evolution, but are responsible only for the redistribution of the conserved quantities. It is important that these properties be preserved when closure schemes are used to approximate the nonlinearity.

The importance of energy and enstrophy conservation is underscored by the role they are believed to play in determining inertial range spectra. It has been argued that the constraint of enstrophy conservation leads to an enstrophy cascade toward small scales in 2-D turbulence, yielding the k^{-1} vorticity spectrum.[11] The constraint of energy conservation is generally believed to yield an inverse cascade toward large scales, and thus a $k^{-5/3}$ energy spectrum.[11] For systems in which the free energy is stored in the largest scale, such as in the finite size shear flows, the inverse cascade manifests itself as the expansion of mean flows. Because this is a slow process, we shall omit the energy evolution from our discussion and primarily focus on the faster enstrophy evolution.

If we consider the inviscid limit, Eq. (6) is useful in describing the way in which vorticity fluctuations evolve under the constraint of enstrophy conservation. The vorticity ρ can be separated into a mean value and a fluctuating part. As discussed in the previous section enstrophy conservation relates the growth of fluctuations to the relaxation of the mean vorticity. Furthermore, the relaxation can be shown to be of the Fokker-Planck type, and thus Eq. (2) becomes

$$\frac{\partial}{\partial t}\int dx\,\langle\delta\rho^2(x)\rangle = \int dx\,\langle\rho\rangle\left[\left(F\frac{\partial}{\partial r}\right)\langle\rho\rangle + \frac{\partial}{\partial r}D\frac{\partial}{\partial r}\langle\rho\rangle\right], \tag{8}$$

where $\mathbf{F}$ and $\mathbf{D}$ are the nonlinear drift and turbulent diffusion coefficients, respectively, and are functions of fluctuation amplitudes. In Sec. IV, we shall return to this point. More

importantly, we shall show that the right-hand side of Eq. (8) is positive definite. Thus, the mean flow indeed tends to relax, and the source for the fluctuation growth is positive.

As discussed in Sec. I, we seek a description of shear flow turbulence which accounts for both wavelike behavior and eddy motion, as well as the interaction of these two elements. It is natural, therefore, in treating shear flow turbulence to attempt to separate the wavelike fluctuation ρ^c and eddy fluctuation $\tilde{\rho}$ from the outset.[30] While such a separation applied directly to vorticity will ultimately prove less useful than a separation of two-point vorticity correlation into wave and eddylike components, it does provide definitions for these two components. We recall that the eddy fluctuation component is intrinsically nonlinear in nature, of small size (in the spanwise direction), and corresponds to the inner solution of the nonlinear critical layer analysis.[16] On the other hand, the wavelike fluctuation component is a nonlinear generalization of the linear response and is similar to the outer solution of the nonlinear critical layer analysis. The definition of each component is obtained by iteration of the vorticity evolution equation, Eq. (4), and identification of contributions to the nonlinearity which are phase coherent with the stream function (wavelike part) and those which are not coherent (eddylike part). This procedure is outlined in what follows. The vorticity fluctuation $\delta\rho$ satisfies

$$\left(\frac{\partial}{\partial t}+V_0(x)\frac{\partial}{\partial y}\right)\delta\rho-\frac{d^2V_0}{dx^2}\frac{\partial\delta\phi}{\partial y}+\frac{\partial\delta\phi}{\partial x}\frac{\partial\delta\rho}{\partial y}-\frac{\partial\delta\phi}{\partial y}\frac{\partial\delta\rho}{\partial x}=0, \tag{9}$$

where the mean flow is $V_0(x)\hat{y}$ and $dV_0/dx=\langle\rho(x)\rangle$. After Fourier transformations in t and y, it follows that

$$\begin{aligned}&-i\left(\omega-kV_0(x)\right)\nabla^2\phi_{k,\omega}-ik\frac{d^2V_0}{dx^2}\phi_{k,\omega}\\&+i\sum_{k',\omega'}\left[ik'\phi_{k',\omega'}\frac{d}{dx}\nabla^2\phi_{k'',\omega''}-ik''\frac{d\phi_{k'',\omega''}}{dx}\nabla^2\phi_{k',\omega'}\right],\end{aligned}$$

where

$$\sum_{k',\omega'}\equiv\frac{1}{4\pi^2}\int dk'\,d\omega'. \tag{10}$$

At this point an iterative method[31] can be applied to renormalize the nonlinear terms.

This method is essentially perturbative in character and assumes that each fluctuation component $f_{k'',\omega''}$ is composed of a primary part $f^{(1)}_{k',\omega'}$, and a driven part $f^{(d)}_{k'',\omega''}$, in which

mode coupling effects are explicitly accounted for. The latter arises from the beating between modes $f^{(1)}_{k,\omega}$ and $f^{(1)}_{-k',-\omega'}$, while the former retains its intrinsic phase. Consequently, the phase-coherent contribution to nonlinear terms in Eq. (10), due to the nonlinear phase build-up, is from $f^{(1)}_{k',\omega'} f^{(d)}_{k'',\omega''}$ and $f^{(d)}_{k',\omega'} f^{(1)}_{k'',\omega''}$, while terms like $f^{(1)}_{k',\omega'} f^{(1)}_{k'',\omega''}$ do not contribute. The iterative operation using the explicit forms of $f^{(d)}_{k'',\omega''}$ (see Eqs. (19)–(22)) then yields both a coherent contribution, which is phase coherent with $f_{k,\omega}$, and an incoherent contribution, which is *not* proportional to $f_{k,\omega}$. Since we are interested primarily in the definitions of ρ^c and $\tilde{\rho}$ at this stage, we do not intend to present the details of the iterative procedure. Some are given in the next section and the Appendix, and the procedure as a whole is described in Refs. (23) and (28). The operators acting on the coherent contribution include both integral operators (nonlocal) and differential operators (local). The nonlocal pieces are related to large-scale interactions. Because their exact physical meaning is obscure, we shall neglect the nonlocal contribution and retain only the local operators that have a clear physical interpretation as turbulent diffusion. In any case, the physical process which we desire to represent in the coherent component is the collective damping which results from turbulent motion. Therefore, the neglect of nonlocal nonlinear effects is not critical in our analysis. In the next section, where the detailed small-scale turbulence structures are addressed in the framework of a two-point formulation, we shall be more careful in treating the nonlinear terms.

The nonlinear terms in Eq. (9) are approximated as

$$-\left[(\nabla\cdot\mathbf{D}\cdot\nabla)\nabla^2\phi_{k,\omega}+i\left(\omega-kV_0(x)\right)\tilde{\rho}_{k,\omega}\right], \tag{11}$$

where $D_{ij}=0$, if $i\neq j$,

$$D_{xx}=\sum_{k',\omega}(k')^2\frac{i\left\langle\phi^2\right\rangle_{k',\omega'}}{\omega''-k''V_0(x)}, \tag{12}$$

$$D_{yy}=\sum_{k',\omega'}\frac{i\left\langle(d\phi/dx)^2\right\rangle_{k',\omega'}}{\omega''-k''V_0(x)}, \tag{13}$$

and

$$\tilde{\rho}_{k,\omega}=-\sum_{k',\omega'}k'\frac{\phi^{(1)}_{k',\omega'}\frac{d}{dx}\left(\nabla^2\phi^{(1)}_{k'',\omega''}\right)-\left(d\phi^{(1)}_{k'',\omega''}/dx\right)\nabla^2\phi^{(1)}_{k',\omega'}}{\omega''-k''V_0(x)}. \tag{14}$$

Since we have used a crude model to account for nonlinearities, we may further approximate the turbulent diffusion by its characteristic time, τ_c, the eddy turnover time. (We shall delay evaluating τ_c until Sec. III.) The incoherent component, which was not retained in previous treatments,[25] is denoted as $\tilde{\rho}$. Now, the total vorticity fluctuation can be separated into the desired form

$$\rho_{k,\omega} = \rho^c_{k,\omega} + \tilde{\rho}_{k,\omega}, \tag{15}$$

where the coherent component ρ^c is

$$\rho^c_{k,\omega} = -k\frac{d^2V_0}{dx^2}\frac{\phi_{k,\omega}}{(\omega - kV_0 + i/\tau_c)}. \tag{16}$$

Note that the coherent component ρ^c is a generalization of linear waves which includes a nonlinear resonance broadening correction. The incoherent component accounts for the filamentary eddies, or the "Cat's eyes," at the wave-flow resonance. Thus, the fast time scale evolution of $\tilde{\rho}$ is simply free convection by the local mean flow.[12] If we approximate $\tilde{\rho}_{k,\omega}$ by $A_k\delta(\omega - kV_0)$, it follows that

$$\nabla^2\phi_{k,\omega} + k\frac{d^2V_0}{dx^2}\frac{\phi_{k,\omega}}{(\omega - kV_0 + i/\tau_c)} = \tilde{\rho}_{k,\omega} = A_k\delta(\omega - kV_0). \tag{17}$$

The stream function ϕ is now approximately proportional to the Green's function of the original linear equation. That is, the nonlinear velocity fluctuations are induced by the seed eddies $\tilde{\rho}$. In turn, the eddies suffer random convection by the turbulent velocity field, and are sheared apart into smaller ones. How this occurs shall ultimately determine the detailed structures of eddies, and is to be discussed next.

III. Two-Point One-Time Vorticity Correlation Equation: Triplet Renormalization

The structure of the incoherent component given in Eq. (14) does not easily permit a tractable analysis of the shearing apart of filamentary eddies under the influence of the turbulent velocity field. Since the eddies are localized, it is natural to formulate a two-point description. As indicated earlier, eddy fluctuations evolve on the slower, turbulent scrambling time scale, so that a two-point, one-time vorticity correlation equation is adequate for capturing the essential evolution of vorticity. In addition to the immense analytical advantage allowed by a two-point formulation, the Fourier components of the two-point correlation function immediately give the spectrum, one of the experimental observables. As with one-point vorticity evolution, the conservation of enstrophy discussed in the previous section imposes a strong condition on the allowed approximations of the nonlinearity. This is in contrast with other amplitude evolution equations whose nonlinear triplets are not subjected to comparison with any constraint.

The ensemble average of the vorticity correlation averages out the fast variation of eddies, and its evolution obeys

$$\left[\frac{\partial}{\partial t}+(V_0(1)-V_0(2))\frac{\partial}{\partial y_-}\right]\langle\delta\rho(1)\delta\rho(2)\rangle$$

$$+\sum_{k',\omega'}e^{ik'y_-}\left\{k'\left[\left\langle\frac{d\phi_{k'',\omega''}}{dx_1}\rho_{k',\omega'}(1)\rho^*_{k,\omega}(2)\right\rangle-\left\langle\frac{d\rho_{k'',\omega''}}{dx_1}\phi_{k',\omega'}(1)\rho^*_{k,\omega}(2)\right\rangle\right]+[1\leftrightarrow 2]^*\right\}$$

$$=\sum_{k,\omega}k\left[\frac{d^2V_0}{dx_1^2}\langle\phi_{k,\omega}(1)\rho^*_{k,\omega}(2)\rangle-\frac{d^2V_0}{dx_2^2}\langle\phi^*_{k,\omega}(2)\rho_{k,\omega}(1)\rangle\right], \tag{18}$$

where molecular viscosity has omitted because it is much smaller than other quantities. It is understood, however, that molecular viscosity always acts on the flows at the smallest length scales. The ensemble average given above can be viewed as a spatial average in the mean flow direction over some distance in the co-moving frame, $y_+ = y_1 + y_2$, or a time average over several periods of fast variation given by the mean flow shear. Therefore, the correlation function is a slowly varying quantity depending weakly on the co-moving frame position, but strongly on the relative position of the two points, $\mathbf{x}_- = \mathbf{x}_1 - \mathbf{x}_2$. Also, the notation $[1 \leftrightarrow 2]^*$ stands for the operation of taking the complex conjugate and interchanging the indices 1 and 2.

To gain some insight into the structure of vorticity correlation, the nonlinear triplets must be approximated. In doing so, the approximation must preserve the basic requirement that the nonlinearity affect no more than a redistribution of the vorticity at various length scales. The triplets contain terms of the form

$$\sum_{k',\omega'} k' \left[\left\langle \frac{d\phi_{k'',\omega''}}{dx_1} \rho_{k',\omega'}(1) \rho^*_{k,\omega}(2) \right\rangle - \left\langle \frac{d\rho_{k'',\omega''}}{dx_1} \phi_{k',\omega'}(1) \rho^*_{k,\omega}(2) \right\rangle \right].$$

The iterative closure scheme used is similar to the DIA (Direct Interaction Approximation) except that the nonlinear propagator, accounting for the amplitude-dependent memory of the fluctuations, is significantly modified by linear phase mixing. The linear phase mixing is actually a more effective means of decorrelating the fluctuations than turbulent mixing. This is apparent from the time scale ordering in which the inverse of the frequency spectrum width is much shorter than the eddy turnover time, as emphasized in the introduction. In this closure scheme, each mode (ρ or ϕ) in the ensemble averaged triplets is driven by the other two modes, and the resulting expression does not depend on the driven modes $\left\langle f_{k',\omega'} f^d_{k'',\omega''} f_{k,\omega} \right\rangle \to \left\langle f^2 \right\rangle_{k',\omega'} \left\langle f^2 \right\rangle_{k,\omega}$, where f^d denotes the driven modes. If only the modes (k'', ω'') and (k', ω') are allowed as driven modes, we then recover the two-point counterpart of the coherent contribution of nonlinear terms discussed in the last section. The incoherent part is obtained from the driven mode (k, ω) in the correlation equation, where the resulting expression does not depend on the amplitude of the mode (k, ω), and corresponds to the incoherent fluctuation. These two contributions to the nonlinear term model a competition of removal and supply of enstrophy within each interval of scales. They are of fundamental importance to this iterative closure scheme, as well as to the DIA. When we sum over all modes and let the two spatial points coincide, the approximated triplets vanish. Then, the total enstrophy evolves without any dependence on nonlinearities. Since comprehensive discussion of the closure scheme has been given in the literature,[31,32] we shall not repeat it, but point out a few essential steps for the shear flow case considered here.

The driven field $\phi^d_{k'',\omega''}$ arising from the beating between modes (k, ω) and $(-k', -\omega')$

satisfies the equation

$$\nabla^2 \phi^d_{k'',\omega''} + k'' \frac{d^2 V_0}{dx^2} \frac{\phi^d_{k'',\omega''}}{(\omega'' - k'' V_0 + i/\tau_c)} = [\mathrm{NL}]_{k'',\omega''},$$

where

$$[\mathrm{NL}]_{k'',\omega''} \equiv \left(\frac{i}{\omega'' - k'' V_0}\right) \cdot \left[k' \left(\frac{d\phi^*_{k',\omega'}}{dx'} \nabla^2 \phi_{k,\omega} - \frac{d\nabla^2 \phi_{k,\omega}}{dx'} \phi^*_{k',\omega'}\right) + (k \leftrightarrow -k')\right]. \quad (19)$$

Hence, $\phi^d_{k'',\omega''}$ can be expressed in terms of a Green's function defined by

$$\nabla^2 G_{k'',\omega''} + k'' \frac{d^2 V_0}{dx^2} \frac{G_{k'',\omega''}}{(\omega'' - k'' V_0 + i/\tau_c)} = \delta(x - x'). \quad (20)$$

We then have

$$\phi^d_{k'',\omega''}(x) = \int dx' G_{k'',\omega''}(x, x') [\mathrm{NL}]_{k'',\omega''}. \quad (21)$$

Thus, the driven vorticity fluctuation $\rho^d_{k'',\omega''}$ satisfies

$$\rho^d_{k'',\omega''}(x) = \int dx' \nabla^2 G_{k'',\omega''}(x, x') [\mathrm{NL}]_{k'',\omega''}. \quad (22)$$

A straightforward, but laborious, substitution of ϕ^d and ρ^d into the triplets of Eq. (18) yields the full expression for the approximated triplet nonlinearities (see Appendix). The time scale for the evolution of the correlation function is on the order of the scrambling time, which is determined by the combination of the relative mean flow shearing and turbulent scrambling on the left side of Eq. (18).

It is of primary interest to examine the situation of stationary turbulence. The stationary solution directly gives the turbulence spectrum and the saturated fluctuation level. The latter is the key quantity for the explanation of turbulent transport. Stationarity of turbulence requires that enstrophy input from the large-scale motion equal enstrophy dissipation at small scale. In order to attain this balance in the highly inviscid limit, sufficient amounts of small-scale fluctuations must be generated. The production of small-scale vorticity fluctuations results in strong vorticity two-point correlation at a small relative separation. Hence, the dominant terms of Eq. (A5) at small separation are the terms with the highest spatial derivatives. The dominant terms have the form of diffusion in the x

and y directions, i.e.,

[Triplets]

$$\approx -\left[\frac{\partial}{\partial x_-}\left(D_{xx}k_0^2y_-^2+D_{yy}k_0^2x_-^2\right)\frac{\partial}{\partial x_-}+\frac{\partial}{\partial y_-}\left(D_{yy}k_0^2y_-^2+D_y''x_-^2\right)\frac{\partial}{\partial y_-}\right]\langle\delta\rho(1)\delta\rho(2)\rangle,$$

where D_{xx} and D_{yy} have been defined in Eqs. (12) and (13),

$$D_y''=\sum_{k',\omega'}\frac{i\left\langle\left|d^2\phi/dx^2\right|^2\right\rangle_{k',\omega'}}{\omega'-k'V_0(x)}, \tag{23}$$

and k_0 is the spectrum averaged wavenumber, given by

$$k_0^2=\frac{\int_0^{y_-^{-1}}dk\,k^4\left\langle\phi^2\right\rangle_{k,kV_0}}{\int_0^{y_-^{-1}}dk\,k^2\left\langle\phi^2\right\rangle_{k,kV_0}}\approx\frac{\int_0^{y_-^{-1}}dk\,k^2\left\langle(d\phi/dx)^2\right\rangle_{k,kV_0}}{\int_0^{y_-^{-1}}dk\left\langle(d\phi/dx)^2\right\rangle_{k,kV_0}}. \tag{24}$$

It is assumed that the dependence of k_0^2 on y_- is weak when y_- is sufficiently small. In the expressions for the D, we can exploit resonance and use the Markovian approximation, whereby the resonant denominator, $1/\left(\omega''-k''V_0(x)\right)$, is replaced by $1/\left(\omega'-k'V_0(x)\right)$. To derive the above expression for the triplets, we have implicitly assumed that the dominant turbulent shear is due to the energetic large-scale wave fluctuations. The full two-point vorticity correlation equation is thus given by

$$\left\{\frac{\partial}{\partial t}+V_0'x_-\frac{\partial}{\partial y_-}-\left[\frac{\partial}{\partial x_-}\left(D_{xx}k_0^2y_-^2+D_{yy}k_0^2x_-^2\right)\frac{\partial}{\partial x_-}+\frac{\partial}{\partial y_-}\left(D_{yy}k_0^2y_-^2+D_y''x_-^2\right)\frac{\partial}{\partial y_-}\right]\right\}$$

$$\cdot\langle\delta\rho(1)\delta\rho(2)\rangle=\sum_{k,\omega}k\left[\frac{d^2V_0}{dx_1^2}\left\langle\phi_{k,\omega}(1)\rho_{k,\omega}^*(2)\right\rangle-\frac{d^2V_0}{dx_2^2}\left\langle\phi_{k,\omega}^*(2)\rho_{k,\omega}(1)\right\rangle\right]\equiv S(1,2), \tag{25}$$

where $V_0'\equiv dV_0/dx$ and $S(1,2)$ stands for the right side of Eq. (18). We note that our approximation of the nonlinear triplets by the relative turbulent diffusion preserves the requirement that it vanish at zero separation. The physical meaning of this result is two-fold: first, the detailed balance between the coherent and incoherent contributions to the nonlinear triplets must be maintained down to the dissipation scale so that small-scale fluctuations are available to couple enstrophy to the dissipation scale; second, the mechanism responsible for this is the differential shearing of eddies by the turbulent flow. To be

precise, the eddy shearing comes from random convection of large-scale motion, hence eddies of very small sizes experience little relative convection and retain their integrity. This explains why the relative turbulent diffusion in Eq. (25) diminishes at a small separation, and small-scale fluctuations thus become populated.

Additional complications result from the structure of the turbulence described by Eq. (25). Here, the mean flow shear participates in the decorrelation of eddies and gives rise to a Fokker-Planck process rather than simple turbulent diffusion. Consequently, the decorrelation rate deviates from that given by homogeneous and isotropic turbulence; and is, in fact, enhanced. This is an important difference between physical situations, and is related to the role of linear phase mixing. Another major difference stems from the way enstrophy is injected from the large-scale sources, as described by $S(1,2)$ in Eq. (25), and is discussed in the next section.

We shall now examine the decorrelation operator given by the left side of Eq. (25). Thus, the characteristic trajectory is a combination of drift and diffusion described by the second-moment Langevin equation

$$\begin{aligned}
\frac{d}{dt}\left\langle y_-^2\right\rangle &= 6k_0^2 D_{yy}\left\langle y_-^2\right\rangle + 2V_0'\left\langle x_- y_-\right\rangle + 2D_y''\left\langle x_-^2\right\rangle \\
\frac{d}{dt}\left\langle x_- y_-\right\rangle &= 4k_0^2 D_{yy}\left\langle x_- y_-\right\rangle + V_0'\left\langle x_-^2\right\rangle \\
\frac{d}{dt}\left\langle x_-^2\right\rangle &= 2k_0^2 D_{xx}\left\langle y_-^2\right\rangle + 4k_0^2 D_{yy}\left\langle x_-^2\right\rangle .
\end{aligned} \tag{26}$$

This set of linear equations can be solved straightforwardly, although the solution is quite tedious. It can also be extended to situations with small but finite viscosity by adding viscosity to the right-hand side of each equation. At the dissipation scale, the solution is very convoluted. Since it is a separate subject we will not attempt to examine it in the present work. There are three eigenmodes of Eq. (26), corresponding to three eigenfrequencies. In general, the solution is a mixture of all three modes, and the component of each mode depends on the initial condition. Fortunately, the solution can be much simplified by considering only the dominant terms at large t. The solution then depends only on the most rapidly growing mode. Assuming that the two components of kinetic energy $k^2\left\langle\phi^2\right\rangle_{k,\omega}$ and $\left\langle(d\phi/dx)^2\right\rangle_{k,\omega}$ are comparable but the vorticity spectrum is highly

anisotropic (see Eqs. (12), (13), and (23)), $k_0^2 D_{yy} \approx k_0^2 D_{xx} \ll D_y''$, and that the mean flow shear is much larger than the turbulent shear $V_0' \gg k_0^2 D_{yy}$, the dominant solution is

$$\begin{aligned}
\left\langle y_-^2(t) \right\rangle &= \frac{1}{3} \exp\left(\frac{t}{\tau_c}\right) \cdot Q_-(0) \\
\left\langle x_-(t) y_-(t) \right\rangle &= \frac{1}{6} V_0' \tau_c \exp\left(\frac{t}{\tau_c}\right) Q_-(0) \\
\left\langle x_-^2(t) \right\rangle &= \frac{1}{6} \left(V_0' \tau_c\right)^2 \exp\left(\frac{t}{\tau_c}\right) Q_-(0),
\end{aligned} \tag{27}$$

where

$$Q_-(0) = \left\langle y_-^2(0) \right\rangle + 2 V_0' \tau_c \left\langle x_-(0) y_-(0) \right\rangle + 2 \left(V_0' \tau_c\right)^2 \left\langle x_-^2(0) \right\rangle \tag{28}$$

and

$$\tau_c = \left[4 k_0^2 D_{xx} \left(V_0'\right)^2\right]^{-1/3}. \tag{29}$$

This solution describes how initially neighboring fluid elements get sheared apart by turbulence. When initial separation is small, it takes longer to separate a sizeable distance. Moreover, we note that the turbulent scrambling time τ_c is proportional to $\left[\left(V_0' k_0\right)^2 D_{xx}\right]^{-1/3}$ which is substantially smaller than that of homogeneous and isotropic turbulence $\left(k_0^2 D_{xx}\right)^{-1}$. The comparison of these two quantities is based on the fact that the mean flow shear is greater than the turbulent shear. It is evident that the mean flow shear can enhance turbulent decorrelation.

IV. Two-Point One-Time Vorticity Correlation Equation: Driving Source

In a 2-D flow, the generation and maintenance of fluctuations occur via the relaxation of mean vorticity gradient, from an unstable configuration toward a stable one. The mean flow does not relax in an arbitrary manner but is constrained by conservation laws, namely, the conservation of total energy and total enstrophy. In particular, the latter stems from a local conservation law, $d\rho/dt = 0$ and is thus a stronger constraint than the global constraint of energy conservation. This local conservation law requires that the vorticity initially associated with a fluid element must remain in the same fluid element during the entire evolution. Therefore, mixing of vorticity is difficult and generally a small eddy can retain its integrity for a time relatively long compared with the lifetime a large eddy. In this section we shall discuss how these individual nonwave objects extract free energy from the mean flow as a result of local conservation of vorticity.

The driving mechanism arises from two distinct processes. First, turbulent velocity fields randomly convect vortices along the mean vorticity gradient, thus bringing together fluid elements of distinct vorticity. This creates local vorticity contrast, i.e., vorticity fluctuations. The second process results from the motion of individual eddies. The principal motion of an eddy is convection in the local mean flow, i.e., $\tilde{\rho}(x,y,t) = \tilde{\rho}\,(x, y - V_0(x)t)$. The second order motion is along the x-direction, with drift speeds dependent on fluctuation amplitudes. Physically, this corresponds to self-induced motion. The direction of the second order motion is such as to enhance the vorticity fluctuations. In other words, a positive vorticity fluctuation (w.r.t. the background) moves up the mean vorticity gradient and a negative one moves down. Both eddy generation processes are tied to the mean flow relaxation, and can be shown as follows:

Since eddies $\tilde{\rho}$ are elongated filaments along the mean flow direction (y-direction), the two-point vorticity correlation function peaks at $x_- = 0$. Moreover, the source term is a smooth function in this limit. Hence, it is convenient to approximate the source term by evaluating it at $x_- = 0$. Thus,

$$S(1,2) \approx S(1,1) = 4 \sum_{k,\omega} k \frac{d^2 V_0}{dx^2} \operatorname{Im} \left\langle \phi_{k,\omega} \rho^*_{k,\omega} \right\rangle .$$

Replacing ρ by ρ^c and $\tilde{\rho}$ from Eqs. (15) and (16), we obtain

$$S(1,1) = 4\sum_{k,\omega} \pi\delta\left(\omega - kV_0(x)\right) k^2 \left\langle \left|\phi_{k,\omega}\right|^2 \right\rangle \left(\frac{d^2V_0}{dx^2}\right)^2$$

$$+ 4\sum_{k,\omega} k\frac{d^2V_0}{dx^2} \operatorname{Im}\left\langle \phi_{k,\omega}\tilde{\rho}^*_{k,\omega} \right\rangle . \tag{30}$$

The first term is easily recognized as the quasilinear diffusion of the mean vorticity, and corresponds to the first relaxation process. The second term will be shown to be the nonlinear drift, and is the second relaxation process. Since the source term is a smooth function and not sensitive to the fine structures of eddies, we can further approximate the incoherent fluctuation $\tilde{\rho}$ by a δ-function

$$\tilde{\rho}_{k,\omega} = A_k(x)\delta\left(\omega - kV_0(x)\right) \tag{31}$$

and

$$\left\langle \tilde{\rho}_{k,\omega}(1)\tilde{\rho}^*_{k,\omega}(2) \right\rangle = \left|A_k\right|^2 \delta\left(\omega - kV_0(x_+)\right) \frac{C(x_-)}{|kV_0'|}, \tag{32}$$

where the structure function $C(x_-)$ is sharply peaked at $x_- = 0$ and can be determined after $\langle\tilde{\rho}\tilde{\rho}\rangle$ is obtained. It is possible to relate the correlation $\left\langle\tilde{\rho}^2\right\rangle$ given in Eq. (32) to the correlation $\langle\phi\tilde{\rho}^*\rangle$ arising in the source term, Eq. (30), using Eq. (17). From Eq. (17), we note that the stream function is given by the Green's function of the Rayleigh equation operating on the seed eddy kernal. The velocity field induced by the seed eddy can now be calculated. When evaluated at the location of the seed eddy, the velocity field accounts for the self-induced motion mentioned earlier. The source term then becomes

$$\begin{aligned} S(1,1) = {} & 4\sum_{k,\omega} \pi\delta\left(\omega - kV_0(x)\right) k^2 \left(\frac{d^2V_0}{dx^2}\right)^2 \left(\frac{|A_k|}{|kV_0'|}\right)^2 \left|G_{k,\omega}\left(x_r, x_r\right)\right|^2 \\ & + 4\sum_{k,\omega} \frac{d^2V_0}{dx^2}\delta\left(\omega - kV_0\right) \frac{|A_k|^2}{|kV_0'|} k \operatorname{Im} G_{k,\omega}\left(x_r, x_r\right), \end{aligned} \tag{33}$$

where x_r is the resonant point, $\omega = kV_0\left(x_r\right)$. In the above expression, we have used the fact that $C(x_-)$ is a strongly peaked function compared with other terms in the integrands, and have approximated it with a $\delta(x_-)$ in the evaluation of the integral $\int dx' \left\langle\tilde{\rho}(x)\tilde{\rho}(x')\right\rangle G(x')$.

Note that the first term on the right-hand side of Eq. (33), the quasilinear diffusion, is positive definite, as in the usual quasilinear theory. The sign of the second term is not

clear at this point. We shall devote the rest of this section to show that it is also positive definite, and that it represents a drift.

To show the positivity of the second term, it is necessary to solve for $\mathrm{Im}\, G(x_r, x_r)$, which ultimately depends on the specific working shear flow profile. Fortunately, if the fluctuation amplitude is not large, i.e., the local resonance width τ_c^{-1} is much smaller than the turbulence spectrum width $\Delta\omega$, $\mathrm{Im}\, G(x_r, x_r)$ can be solved for approximately. From Eq. (20), we have

$$\nabla^2 G_{k,\omega}(x, x_r) + k\frac{d^2V_0}{dx^2}\left[\frac{(\omega - kV_0)}{(\omega - kV_0)^2 + 1/\tau_c^2} - \frac{i/\tau_c}{(\omega - kV_0)^2 + 1/\tau_c^2}\right] G_{k,\omega}(x, x_r) = \delta(x - x_r), \tag{34}$$

where the resonant denominator has a sharp negative imaginary part. Now we multiply both sides of the equation by $G^*(x, x_r)$, and integrate over x from $-\infty$ to ∞. Separating the imaginary part from the real part, we obtain $\mathrm{Im}\, G(x_r, x_r)$ immediately,

$$\mathrm{Im}\, G_{k,\omega}(x_r, x_r) = \pi\frac{d^2V_0}{dx_r^2}\left(\frac{k}{|kV_0'|}\right)|G_{k,\omega}(x_r, x_r)|^2 .$$

Hence, the second term of Eq. (33) now becomes identical to the first term and is positive definite. Furthermore, since $\mathrm{Im}\, G$ is proportional to $\mathrm{Im}\,\phi$, $k\,\mathrm{Im}\, G(x_r, x_r)$ is proportional to δV_x, the velocity field in the x-direction. That is,

$$\delta v_x = -\frac{\partial\phi}{\partial y} = \sum_k k\,\mathrm{Im}\,\phi_{k,kV_0} \propto \sum_k A_k k\,\mathrm{Im}\, G_{k,kV_0} \propto \sum_k A_k\frac{d^2V_0}{dx_r^2}. \tag{35}$$

Note that if $A_k > 0$, the eddy moves up the vorticity gradient, whereas if $A_k < 0$, then it moves down the vorticity gradient. Finally, the two contributions to the source term for eddy fluctuations turn out to be positive and equal. That is,

$$S(1,1) = 8\sum_{k,\omega}\pi\delta(\omega - kV_0(x))\,k^2\left(\frac{d^2V_0}{dx^2}\right)^2\left(\frac{A_k}{kV_0'}\right)^2|G_{k,\omega}(x_r, x_r)|^2 . \tag{33'}$$

This is related to the fact that eddies of the like sign attract each other, making regular and smooth distributions less favorable. The source which drives localized fluctuations is always positive, so that flows tend to clump. This vortex collapse is a well known phenomenon

in 2-D turbulence. It is instructive to compare this result with that for a similar system, the 1-D Vlasov electron plasma.[33] In the electron phase space, the electron distribution function is sheared by the particle velocity just as the vorticity is in a shear flow. But the electron phase-space clumps cannot persist because the source term vanishes due to a cancellation between the diffusion and the drift. This opposite behavior is primarily due to the fact that electrons repel, rather than attract each other, and the system is thus more amenable to smooth and uniform distributions.

V. Correlation Function, Spectrum and Saturation Level

Having shown the positivity of the source which drives small-scale eddies, and having obtained a description for the turbulent shearing apart of eddies, we now turn to examine some features of stationary turbulence. In particular, we are interested in the spectrum and the saturated fluctuation level.

(a) Vorticity correlation function and spectrum

The vorticity correlation function can, in principle, be solved by inverting the Fokker-Planck operator of Eq. (25). For stationary turbulence, the source is effectively propagated forward in time by the inverse Fokker-Planck operator, or equivalently, the coordinates of the source can be propagated backward in time. This familiar procedure was first used in fluid turbulence problems by Batchelor[34] and later in plasma turbulence problems by Dupree.[30] These two equivalent methodologies are often referred to as Eulerian and Lagrangian pictures.

The fluid-element trajectories are stochastic due to overlapping of cat's-eyes. Any two nearby elements diverge from each other exponentially rapidly in time, as shown in Sec. III. The time constant depends on the fluctuation level, and is approximately equal to the nonlinear scrambling time τ_c. The stationary vorticity correlation function can be obtained by propagating fluid trajectories backward in time using Eq. (27). The solution is

$$\langle \delta\rho(1)\delta\rho(2)\rangle = \tau_{\rm eddy}(\mathbf{x}_-)S(1,1), \tag{36}$$

where $\tau_{\rm eddy}(\mathbf{x}_-)$, the eddy lifetime, depends primarily on the sizes of eddies as measured by the separation of fluid elements $\mathbf{x}_-$. In the Lagrangian picture, $\tau_{\rm eddy}$ is a measure of

the amount of time spent by two nearby fluid elements of initial separation $\mathbf{x}_-$ in diverging a distance equal to the typical turbulence length scale, k_0^{-1}. Since small eddies experience little relative shearing by large-scale convection, their eddy lifetime is long relative to large eddies. Therefore, $\tau_{\text{eddy}}(\mathbf{x}_-)$ peaks at $\mathbf{x}_- = 0$. In the Eulerian picture, the equivalent statement is that vorticity is highly correlated at a small separation, as is evident from Eq. (36).

The derivation of Eq. (36) was first given by Dupree[30] in the Vlasov turbulence context, and will not be repeated here. The expression for $\tau_{\text{eddy}}(\mathbf{x}_-)$ can be obtained from the above definition

$$k_0^2 \left[y_- \left(t = \tau_{\text{eddy}}\right)\right]^2 = 1, \tag{37}$$

with the initial separation given by x_- and y_-. From Eq. (27), it follows that

$$\tau_{\text{eddy}}(\mathbf{x}_-) = \tau_c \ln \left\{ \frac{3/k_0^2}{y_-^2 - 2V_0'\tau_c x_- y_- + 2\left(V_0'\tau_c x_-\right)^2} \right\}. \tag{38}$$

The lifetime is logarithmically singular for infinitesimally small eddies. At the smallest scales, however, viscosity actually cuts off the singularity.[35] This expression is similar to the clump lifetime of the "phase space eddies" of one-dimensional Vlasov plasmas.[30] This is primarily because the dominant long-time dynamics of both kinds of eddies is controlled by velocity diffusion. In the case of Vlasov-plasma eddies, the diffusion occurs in phase space, while for fluid eddies it occurs in real space.

The incoherent-fluctuation piece $\langle\tilde{\rho}(1)\tilde{\rho}(2)\rangle$ of the vorticity correlation function can be obtained by subtracting the coherent portion from $\langle\rho(1)\rho(2)\rangle$. The coherent portion arises from scattering of waves by the trapped vortex elements ballistically propagating at wave phase velocities. It is given approximately by $\tau_c S(1,1)$.[33] Therefore,

$$\begin{aligned}
\langle\tilde{\rho}(1)\tilde{\rho}(2)\rangle &= \left[\tau_{\text{eddy}}(\mathbf{x}_-) - \tau_c\right] S(1,1) \\
&\cong \tau_c \ln \left\{ \frac{1/k_0^2}{y_-^2 - 2V_0'\tau_c x_- y_- + 2\left(V_0'\tau_c x_-\right)^2} \right\} S(1,1) \qquad (39) \\
&= 0, \qquad \text{otherwise.}
\end{aligned}$$

We remind ourselves that approximations made in deriving the expression for the two-point vorticity correlation function, Eq. (25), are intended for the investigation of small-scale

vorticity fluctuations, i.e., $\langle\tilde{\rho}(1)\tilde{\rho}(2)\rangle$. Fourier transforming Eq. (39), we have

$$\langle\tilde{\rho}(1)\tilde{\rho}(2)\rangle_{\mathbf{k}} = \left(\frac{2}{|V_0'|}\right)\left(\frac{1}{p^2}\right)\left[1 - J_0\left(\frac{\sqrt{2}p}{k_0}\right)\right]\cdot S(1,1), \tag{40}$$

where

$$p^2 = (k\cos\theta + q\sin\theta)^2 + \frac{1}{4}\left(V_0'\tau_c\right)^2(k\sin\theta - q\cos\theta)^2,$$

$k = k_y$, $q = k_x$, and J_0 is the zero order Bessel function. A typical equi-p contour is a tilted elongated ellipse as shown in Fig. 1.

Although the vorticity spectrum is anisotropic due to mean flow shear V_0', the spectrum is basically proportional to $1/\left(k^2+q^2\right)$ for large k and q. This fact indicates that the self-similar enstrophy cascade does occur, but it is affected by mean flow shear and becomes anisotropic. It should be emphasized again that the vorticity correlation equation, Eq. (25), is obtained under the assumption that turbulent shear is determined primarily by nonlocal (in wavenumber space) interaction with large-scale $\left(\geq k_0^{-1}\right)$ fluctuations.

At the low-$\mathbf{k}$ end of the vorticity spectrum (see Fig. 2), we have Eq. (40). The oscillation due to the Bessel's function in the high-$\mathbf{k}$ limit is introduced by the artificial cutoff of Eq. (39) and is unphysical. The presence of J_0, nonetheless, tends to flatten the low-$\mathbf{k}$ spectrum, thus it reflects the absence of long-range eddy correlation. Since the range of validity of the anisotropic spectrum sensitively depends on the relative amplitudes of large-scale ($k \leq k_0$) fluctuations to those of small-scale fluctuations, it is desirable to determine the spectral shape of vorticity fluctuations in the low-k regime. This, however, is a difficult task because it depends on the detailed balance of the excitation of individual wave fluctuations and their nonlinear couplings, and defies generalization which would otherwise make it amenable to analytical treatments.

Nonetheless, numerical calculations[36] have produced evidence that a spectral "bump" occurs below the inertial range for plane jets (and wakes). This result is important because it justifies our assumption of the existence of energetic low-k fluctuations. A typical vorticity $\mathbf{k}$-spectrum with spectral anisotropy is shown in Fig. 2. The low-$\mathbf{k}$ spectral bump (solid line) is due to the excitation of fluctuations near wave resonances. The wavenumber k_1, where the predicted anisotropic spectrum $\left(\sim p^{-2}\right)$ no longer holds and a logarithmic

correction is needed, can be estimated by equating the contribution to turbulent shear from the spectral bump to that of the cascade range. That is,

$$\int_0^{\bar{k}} dk\Omega(k) \sim \int_{\bar{k}}^{k_1} dk\Omega(k) \sim \bar{k}\Omega(\bar{k}) \ln \frac{k_1}{\bar{k}},$$

where $\Omega(k) \equiv k^4 \left\langle \phi^2 \right\rangle_k$, and $\bar{k}$ is the wavenumber which separates the spectral bump from the anisotropic cascade range and is slightly larger than k_0. Hence,

$$k_1 \sim \bar{k} \exp \left\{ \frac{\int_0^{\bar{k}} dk\Omega(k)}{\bar{k}\Omega(\bar{k})} \right\}. \tag{41}$$

The break k_2, where the logarithmically corrected anisotropic spectrum becomes isotropic, can be determined by equating turbulent shear to mean flow shear. Unfortunately, it cannot be determined without solving for the logarithmically corrected anisotropic spectrum. Since this is a separate subject, we will not discuss it further in the present work.

(b) Saturation level

Now we focus on the spectral bump; in particular, we are interested in where it is located and how much energy it contains. In the low-k regime, the total vorticity spectrum is modified by the presence of energetic wave fluctuations. However, incoherent fluctuations, which are generated by nonlinear mode coupling, may still follow the cascade spectrum, Eq. (40), all the way to $k \approx k_0$. In the vorticity contour plots of Zabusky's simulations, the low-k incoherent fluctuations are recognizable as slender, concentrated vortex filaments and are distinguishable from round rolls of wave fluctuations. The relation between wave fluctuations and incoherent fluctuations is given by Eq. (17) which states that the total fluctuation $\delta\rho^c + \tilde{\rho}$ is induced by seed incoherent fluctuations $\tilde{\rho}$. Note that the total fluctuation can be significantly enhanced when the frequency is near the collective resonance, $\omega(k)$, defined by the homogeneous solutions of Eq. (17) which in turn correspond to the resonances of the Green's function defined in Eq. (20). Using Eqs. (32), (33′), and (38), and noting that the Green's function contains the amplitude-dependent τ_c, we may construct a nonlinear amplitude equation. To determine the fluctuation level it is convenient to write an equation for $S(1,1)$ rather than for A_k^2 or $\langle\tilde{\rho}\tilde{\rho}\rangle$. Using Eq. (32),

and realizing that $\langle\tilde{\rho}(1)\tilde{\rho}(2)\rangle_{k,\omega} = 2\pi\delta\left(\omega - kV_0\left(x_r\right)\right)\langle\tilde{\rho}(1)\tilde{\rho}(2)\rangle_k$, we have

$$S(1,1) = 4\int dk \int d\omega\delta\left(\omega - kV_0(x)\right)\left(\frac{V_0''}{V_0'}\right)^2 \left|G_{k,\omega}\left(x_r, x_r\right)\right|^2 \cdot \left[1 - J_0\left(\frac{\sqrt{2}k}{k_0}\right)\right] S(1,1). \tag{42}$$

$S(1,1)$ is common to both sides and can be cancelled. The dominant amplitude dependence in Eq. (44) is contained in $G_{k,\omega}$, near collective resonance. Near collective resonance, $G_{k,\omega}^{-1}$ can be expressed as

$$G_{k,\omega}^{-1}\left(x_r\right) = \left[\omega + \frac{i}{\tau_c} - \omega(k)\right]\frac{\partial G_{k,\omega}^{-1}}{\partial\omega} \tag{43}$$

hence,

$$\left|G_{k,\omega}\left(x_r\right)\right|^2 = \frac{\left|\partial G_{k,\omega}^{-1}/\partial\omega\right|^{-2}}{\left(\omega - \omega_r(k)\right)^2 + \left(1/\tau_c - \omega_i(k)\right)^2}, \tag{44}$$

where ω and k are taken to be real, but the linear eigenfrequency $\omega(k)$ is complex. Since $\left|G_{k,\omega}\left(x_r\right)\right|^2$ is small unless ω is near $\omega_r(k)$, the ω integral in Eq. (44) is dominated by the contribution near collective resonance. That is,

$$1 = 4\pi\int dk\delta\left(kV_0(x) - \omega_r(k)\right)\left(\frac{V_0''}{V_0'}\right)^2\left[1 - J_0\left(\frac{\sqrt{2}k}{k_0}\right)\right]\frac{\left|\partial G_{k,\omega}^{-1}/\partial\omega\right|^{-2}}{1/\tau_c - \omega_i(k)}\Bigg|_{\omega=\omega_r(k)}. \tag{45}$$

The k-integral can be evaluated at the wave-flow resonances, $\omega_r(k)/k = V_0(x)$, where the phase velocity locally matches the mean flow velocity. It states that only those filamentary eddies whose ballistically propagating speed matches the wave phase velocity can yield enhanced fluctuations. Physically, an eddy must be trapped by the roll-up motion of wave fluctuations in order to have enough time to precipitate wave evolution. Once an eddy is trapped, its momentum, given by the mean flow convection, can be deposited onto the roll-up motion, thus stretching the spiral arms and enhancing the wave fluctuations. Consequently, the condition for stationary shear flow turbulence becomes

$$\frac{1}{\tau_c}(x) = \left\{\omega_i(k) + 6\left|\frac{\left(V_0''\right)^2}{\left(V_0'\right)^3}\right|\left|\frac{\partial G_{k,\omega}^{-1}}{\partial\omega}\right|^{-2}\right\}\Bigg|_{\substack{\omega=\omega_r(k)\\ k=k_0(x)}}, \tag{46}$$

where $k_0(x) \equiv \left(\omega_r\left(k_0\right)\right)/\left(V_0(x)\right)$.

The conventional method[25] for the estimation of fluctuation amplitudes argues that the amplitude-dependent turbulent diffusion must offset linear growth rates in order to achieve stationary turbulence. Hence, $1/\tau_c = \omega_i(k)$. The additional positive term in Eq. (46) accounts for the relaxation of mean flow vorticity on the nonlinear time scale, which tends to enhance vorticity fluctuations.

Notice that τ_c varies with position. At the inflection points, $V_0'' = 0$ and $\omega_i\left(k_0(x)\right) = 0$, because the wave-flow resonances at the inflection points yield neutral solutions. Therefore, $1/\tau_c$ is vanishingly small at the inflection points. However, the pole-approximations for wave-flow resonances used above actually have finite widths, hence $1/\tau_c$ may not vanish, but rather have local minim at the inflection points. We also note that ω_i can be negative for sufficiently large k. Usually, the locations of flow resonances $\left(V_0(x) = \omega_r/k\right)$ with negative ω_i and those with positive ω_i are divided by the inflection points. Because $|G_{k,\omega}|^2$ is fairly uniform across the flow, the locations with negative ω_i may thus have smaller $1/\tau_c$.

Using Eqs. (12) and (29), and the fact that $1/2\pi \int dk k^2 \left\langle \phi^2 \right\rangle_{k,kV_0} \sim \omega_r\left(k_0\right) \left\langle \delta v_x^2 \right\rangle$, we now obtain an estimate for $\left\langle \delta v_x^2 \right\rangle$,

$$\left\langle \delta v_x^2 \right\rangle \sim \frac{\omega_r\left(k_0\right)}{4\left(k_0 V_0'\right)^2} \left\{ \omega_i\left(k_0\right) + 6\frac{\left(V_0''\right)^2}{\left|V_0'\right|^3} \left| \frac{\partial G_{k_0,\omega}^{-1}}{\partial \omega} \right|^2 \right\}^3 \Bigg|_{\omega=\omega(k_0)} . \tag{47}$$

An accurate estimate for $\left\langle \delta v_x^2 \right\rangle$ depends on specific working profiles which primarily affect the second term on the right. Here, we seek to estimate the lower bound of $\left\langle \delta v_x^2 \right\rangle$ for plane jets or wakes by keeping only $\omega_i\left(k_0\right)$ in Eq. (47). For a typical maximum growth rate, $\omega_i \sim 0.2U_0/a$ (where U_0 and a are maximum flow speed and the flow width, respectively), the typical real frequency, mean flow shear and wavenumber are $\omega_r \sim 0.6U_0/a$, $V_0' \sim 0.6U_0/a$, and $k \sim 1/a$. Thus, the lower bound of $\left\langle \delta v_x^2 \right\rangle$ is

$$\left\langle \delta v_x^2 \right\rangle_{\text{l.b.}} \sim 4 \times 10^{-3} U_0^2,$$

for typical plane jets and wakes. When compared with the numerical results of Zabusky et al., the estimated lower bound of $\left\langle \delta v_x^2 \right\rangle$ is one order of magnitude smaller. This indicates that the second term in Eq. (47) can be comparable to ω_i.

Here, we want to stress the physical significance of the amplitude enhancement, i.e., the second term in Eq. (47). This term can be traced back to the eddy lifetime, τ_{eddy}, from

Eqs. (39), (40), and (45), which in turn arises from the inversion of the Fokker-Planck operator in the relative coordinate (cf. Eq. (25)). The relative diffusion in Eq. (25) represents mode coupling and enstrophy cascade. Thus, the enhancement of saturation levels arises from the excitation of high-k modes, which are linearly stable, by mode coupling. In this regard, the conventional saturation estimate, i.e., retaining only the first term in Eq. (47), is misleading, in that it only accounts for the amplitudes of the large-scale linearly unstable waves but fails to account for the contribution from smaller-scale fluctuations. Note that saturation of linearly unstable waves is due to beating of unstable modes (the first term in Eq. (47)) and consequently transfer of fluctuation energy to high-k modes (the second term). The two are closely related, and should *both* contribute to the total saturation level.

VI. Summary and Conclusions

We have presented a description of 2-D shear flow turbulence which includes vortex filaments (eddies) and linearly unstable modes, both of which naturally arise in unstable shear flows. In the presence of a sheared mean flow, large vortex filaments arise from the mode coupling of linearly unstable modes. Such eddies extract enstrophy available in the mean flow. Turbulent scattering processes then transfer the enstrophy to smaller scales. In contrast to homogeneous and isotropic turbulence, turbulent scrambling of eddies by large-scale, spatially smooth wave fluctuations plays an important role. A critical wavenumber $k_\perp$ effectively separates regions of the spectrum in which transfer of enstrophy by wave-eddy interactions dominates and regions in which more conventional eddy–eddy interactions dominate the transfer process. For scales which are larger than k_1^{-1}, the dominant shearing force consists of large-scale wave fluctuations whose characteristics and structure are determined by the mean flow profile. Smaller eddies in this range undergo slower turbulent decay because they experience little relative turbulent shearing by large-scale eddies. Eddies tend to be anisotropic as a consequence of the role played by the mean flow in the turbulent scattering process. For scales which are smaller than k_1^{-1}, the influence of the mean flow shear is minimal and eddy fluctuations provide the dominant contribution to the enstrophy transfer process (eddy–eddy scattering). Here the eddy

turnover rate is somewhat faster and the eddies tend to be isotropic.

It has also been shown that large eddies tap free energy from the mean flow in a nonlinear process which differs fundamentally from energy extraction by linearly unstable modes. Two mechanisms are involved. First, the turbulent scattering of mean flow vorticity shuffles the large-scale, smooth mean flow vorticity into vortex fluctuations (quasilinear diffusion). Second, individual eddies induce nonlinear drifts in the span-wise direction so as to enhance the local fluctuation level, at the expense of mean flow vorticity flattening. The nonlinear drift is such that positive vortices tend to drift to the positive vorticity side and vice versa. Both the quasilinear diffusion and nonlinear drift contributions are positive definite and add to yield a positive total free energy source.

In the steady state, the fluctuation energy removal by cascade toward dissipative scales and the free energy extraction from mean flows must reach a balance. This ultimately requires a certain fluctuation amplitude and permits an estimate of the saturation level. This estimate can be significantly larger than that obtained using conventional methods, in which the amplitude-dependent turbulent diffusion is balanced with linear growth rates.

The theory assumes that the linear dephasing time scale $1/\Delta\omega$ is small in comparison to the nonlinear scrambling time τ_c. This condition holds if the fluctuation amplitudes are not too large. For typical plane jets and wakes, the ratio of the linear dephasing time to the nonlinear scrambling time is calculated to be about $1/3$ or less. Nevertheless, higher order corrections tend to reduce this ratio somewhat. Hence, our predictions are still reliable but should be interpreted with caution. For example, one cannot apply this theory to mixing layer flows, for they have relatively small ranges of real frequencies and the expansion is not valid.

The theory highlights the different roles played by eddy–eddy interactions and by wave–eddy interactions, within a statistical framework. In addition, the theory naturally leads to an anisotropic vorticity spectrum and bridges the transition between mean flows, the free energy source, and the fine-scale isotropic inertial range. The theory predicts that the locations of the minima $\langle \delta v_x^2 \rangle$ occur at the inflection points of the mean flows. This is because the eddy-generation source, V_0'', locally vanishes, and hence no eddy is available to induce wave fluctuations. Unfortunately, experimental and numerical measurements for

the spatial variation of $\langle \delta v_x^2 \rangle$ have not been adequate to clearly determine its structure. (Most measurements have been of $\langle \delta v_y^2 \rangle$, or for 3-D turbulence.) The only 2-D numerical results for $\langle \delta v_x^2 \rangle$, as far as we are aware, are those of Aref and Siggia.[36] They simultaneously showed mean flow and $\langle \delta v_x^2 \rangle$ profiles at different times during the evolution in an attempt to demonstrate that the general structure of the mean flow and $\langle \delta v_x^2 \rangle$ follow certain scaling laws. However, in the course of nonlinear evolution the flow expanded, finite boundary effects became important, and the mean flow profiles became very irregular. Not only were the inflection points difficult to locate precisely, but the flow seemed to have several inflection points at that stage. Although the profiles of $\langle \delta v_x^2 \rangle$ appear to have several minima, they do not seem to be well correlated with the locations of inflection points using visual examination. Thus, we believe that a numerical simulation with a frozen mean flow is necessary to circumvent the finite-boundary effects. By such a method, the resulting detailed structures may be more reliable and suitable for comparison with the theoretical predictions.

Also we note that the prediction of minimum turbulent diffusion at the inflection points differs from the so-called "variable-eddy-viscosity" formula[38] for three-dimensional turbulence. In this formula, the Reynolds stress, $\langle \delta v_x \delta v_y \rangle$, is proportional to dV_0/dx which has a maximum (or minimum) at the inflection point. We believe that the three dimensionality, which breaks the vorticity conservation law, is responsible for this difference. It is also interesting to point out that, from the visual displays of vortex evolution in a 2-D simulation,[20] the round rolls (which we interpret as a composite of wave and eddy fluctuations) seem to be located off the center of jet flows, and that the central fluctuations are dominated by filamentary vortices. They can be explained by our theory as follows. Near the center of the jet flow the resonance phase velocity, $\omega(k)/k = V_0(x)$, is too high to be consistent with unstable modes. Thus, waves are damped and only eddies that are scattered by waves toward the center are present.

The picture of shear flow turbulence in terms of interactions between eddies and waves is not new. In the numerical work of Zabusky and Deem,[35] it was reported that elliptical rolls appeared to nutate about the flow direction at a very low frequency. This phenomenon may be interpreted as the beating of two comparable scale wave fluctuations.

Furthermore, vortex merging also points to the significance of wave fluctuations. As the mean flow expands, the most linearly unstable modes shift to lower k values. The vortices are thus bunched together by the longer wavelength modes. These, however, are all large-scale coherent vortices and are beyond the description of the present statistical theory of small-scale vortices.

Despite the emphasis of this work on the interactions between wave and eddy fluctuations, the existence of linearly unstable wave fluctuations is not essential to this theory. In other words, shear flow turbulence can be comprised of eddies just like isotropic turbulence. This idea has been put forth by Townsend[12] in his Rapid-Distortion theory. However, it is not clear from that theory why the fluctuation-energy production term, i.e., $-\langle \delta v_x \delta v_y \rangle \, dV_0/dx$, should be positive. In our theory we have shown that the net enstrophy transfer from the mean flow to fluctuations is positive definite.

An important implication of this study is the possibility of turbulence in the absence of inflection points, and thus in the absence of unstable collective resonances. This route to turbulence is a consequence of the fact that linear theories are only valid for a short time. On a long time scale, nonlinearity, even if small, can participate in the dynamics and play an important role. The long-time dynamics are governed by, among other things, the two-point vorticity correlation equation from which we obtain Eq. (44). Without collective resonances, Eq. (44) can still be satisfied. This equation requires the enstrophy output to be balanced by enstrophy input. When the equation is satisfied, the existence of turbulence is possible. However, the extension to this regime from the present study is nontrivial. Difficulties arise in accounting for the nonlocal interactions (in $\mathbf{k}$ space), which lead to the log-corrected spectrum.

Free shear flows without inflection points are rare in controlled experiments. However, in many astronomical objects they do exist, e.g., in accretion disks.[28] In galaxies, the mechanism of accretion of matter into compact objects, such as black holes, remains controversial. In the highly dissipationless astronomical environments, conservation of angular momentum is a strong constraint that prevents accretion. It has been suggested[39] that turbulent dissipation is responsible for the redistribution of angular momentum and thus for matter accretion. For thin disks, the rotation velocity obeys Kepler's laws because

self-gravitation and pressure are both negligible. As a result, the disk angular momentum increases outward monotonically. For two-dimensional fluctuations, which are appropriate if length scales are greater than the disk thickness, this kind of angular momentum profile is stable. Actually, collective resonances do not even exist due to the lack of angular momentum extrema, the counterparts of inflection points in a cylindrical coordinate. Extension of the present work to the "waveless" regime is therefore not only practical but also relevant to this long-standing problem in astrophysics.

Acknowledgements

We are happy to acknowledge support by NSF Grant #ATM 8506632 and DOE Grant #DE-FG05-80ET-53088. T. C. would like to thank E. G. Zweibel for useful suggestions.

Appendix: Renormalization of Triplet Terms

In the following, we shall show that the triplet correlation in Eq. (18) can be approximated by a relative diffusion of the vorticity correlation, and a term which can be written as a total derivative with respect to x. The latter serves as a nonlinear source for the vorticity correlation. The iteration scheme is that used in a previous work.[25] The triplet correlation can be expressed in terms of the second order driven field and vorticity as

$$
\begin{aligned}
i\sum_k \Bigg\{ & \left[k' \left\langle \frac{d\phi^{(d)}_{k''}(1)}{dx_1} \rho_{k'}(1)\rho^*_k(2) \right\rangle + k'' \left\langle \phi^{(d)}_{k''}(1) \frac{d\rho_{k'}(1)}{dx_1} \rho^*_k(2) \right\rangle \right] \\
& + \left[k'' \left\langle \frac{d\phi_{k'}(1)}{dx_1} \rho^{(d)}_{k''}(1)\rho^*_k(2) \right\rangle + k' \left\langle \phi_{k'}(1) \frac{d\rho^{(d)}_{k''}(1)}{dx_1} \rho^*_k(2) \right\rangle \right. \\
& \left. + k \left\langle \frac{d\phi_{k'}(1)}{dx_1} \rho_{k''}(1)\rho^{*(d)}_k(2) \right\rangle + k' \left\langle \phi_{k'}(1) \frac{d\rho_{k''}(1)}{dx_1} \rho^{*(d)}_k(2) \right\rangle \right] \Bigg\} \\
& + \{1 \leftrightarrow 2\}^* .
\end{aligned}
\tag{A1}
$$

Here, each of $\phi(1)$, $\phi(2)$, $\rho(1)$, and $\rho(2)$ can be a driven mode, and $\phi(1), \ldots$, etc., represents $\phi(x_1), \ldots$, etc., respectively. The notation $\{1 \leftrightarrow 2\}^*$ represents the complex conjugate of the previous terms in the brace, with positions x_1 and x_2 interchanged.

To avoid the unnecessary complication associated with the spatial derivatives of driven modes ($d\phi^{(d)}/dx$ and $d\rho^{(d)}/dx$), they are extracted as follows:

$$
\begin{aligned}
\frac{d\phi^{(d)}_{k''}(1)}{dx_1} \rho_{k'}(1)\rho^*_k(2) = & \left[\frac{d}{dx_1} \left(\phi^{(d)}_{k''}(1)\rho_{k'}(1)\rho^*_k(2) \right) - \phi^{(d)}_{k''}(1)\rho_{k'}(1) \frac{d\rho^*_k(2)}{dx_2} \right] \\
& + \phi^{(d)}_{k''}(1) \left[\rho_{k'}(1) \frac{d\rho^*_k(2)}{dx_2} - \frac{d\rho_{k'}(1)}{dx_1} \rho^*_k(2) \right]
\end{aligned}
\tag{A2}
$$

and

$$
\begin{aligned}
\phi_{k'}(1) \frac{d\rho^{(d)}_{k''}(1)}{dx_1} \rho^*_k(2) = & \left[\frac{d}{dx_1} \left(\phi_{k'}(1)\rho^{(d)}_{k''}(1)\rho^*_k(2) \right) - \phi_{k'}(1)\rho^{(d)}_{k''}(1) \frac{d\rho^*_k(2)}{dx_2} \right] \\
& + \left[\phi_{k'}(1)\rho^{(d)}_{k''}(1) \frac{d\rho^*_k(2)}{dx_2} - \frac{d\phi_{k'}(1)}{dx_1} \rho^{(d)}_{k''}(1) \frac{d\rho^*(2)}{dx_2} \right].
\end{aligned}
\tag{A3}
$$

After rearrangement, it is straightforward to substitute $\phi^{(d)}$ and $\rho^{(d)}$ from Eqs. (21) and (22), yielding that

$$[\text{Triplet}] = \left\{ \left[\frac{d}{dx_1} + \frac{d}{dx_2} \right] A(1,2) + B_1 + B_2 + B_3 \right\} + \{1 \leftrightarrow 2\}^*, \qquad (A4)$$

where

$$A(1,2) = \sum_{\substack{k',\omega' \\ k,\omega}} \int dx' \Bigg\{ \left(\frac{i}{\omega'' - k''V_0} G_{k'',\omega''}(1,x') \right)$$

$$\cdot (k')^2 \Bigg[\left\langle \rho_{k',\omega'}(1) \rho^*_{k',\omega'}(x') \right\rangle \left\langle \frac{d\phi_{k,\omega}(x')}{dx'} \rho^*_{k,\omega}(2) \right\rangle$$

$$- \left\langle \rho_{k',\omega'}(1) \phi^*_{k',\omega'}(x') \right\rangle \left\langle \frac{d\rho_{k,\omega}(x')}{dx'} \rho^*_{k,\omega}(2) \right\rangle \Bigg] - \left(\frac{i}{\omega'' - k''V_0} \nabla^2 G_{k'',\omega''}(1,x') \right)$$

$$\cdot (k')^2 \Bigg[\left\langle \phi_{k',\omega'}(1) \rho^*_{k',\omega'}(x') \right\rangle \left\langle \frac{d\phi_{k,\omega}(x')}{dx'} \rho^*_{k,\omega}(2) \right\rangle$$

$$- \left\langle \phi_{k',\omega'}(1) \phi^*_{k',\omega'}(x') \right\rangle \left\langle \frac{d\rho_{k,\omega}(x')}{dx'} \rho^*_{k,\omega}(2) \right\rangle \Bigg] \Bigg\},$$

$$B_1 = - \sum_{\substack{k',\omega' \\ k,\omega}} \int dx \Bigg\{ k^2 \left(\frac{i}{\omega'' - k''V_0} \nabla^2 G_{k'',\omega''}(1,x') \right)$$

$$\cdot \Bigg[\left\langle \frac{d\phi_{k',\omega'}(1)}{dx_1} \frac{d\phi^*_{k',\omega'}(x')}{dx'} \right\rangle \left\langle \rho_{k,\omega}(x') \rho^*_{k,\omega}(2) \right\rangle$$

$$- \left\langle \frac{d\phi_{k',\omega'}(1)}{dx_1} \frac{d\rho^*_{k',\omega'}(x')}{dx'} \right\rangle \left\langle \phi_{k,\omega}(x') \rho^*_{k,\omega}(2) \right\rangle \Bigg] - (k'')^2 \left(\frac{i}{\omega - kV_0} \nabla^2 G^*_{k,,\omega}(2,x') \right)$$

$$\cdot \Bigg[\left\langle \frac{d\phi_{k',\omega'}(1)}{dx_1} \frac{d\phi^*_{k',\omega'}(x')}{dx'} \right\rangle \left\langle \rho^*_{k'',\omega''}(x') \rho_{k'',\omega''}(1) \right\rangle$$

$$- \left\langle \frac{d\phi_{k',\omega'}(1)}{dx_1} \frac{d\rho_{k',\omega'}(x')}{dx'} \right\rangle \left\langle \phi^*_{k'',\omega''}(x') \rho_{k'',\omega''}(1) \right\rangle \Bigg] \Bigg\},$$

$$B_2 = \sum_{\substack{k',\omega' \\ k,\omega}} \int dx' (k')^2 \Bigg\{ \left(\frac{i}{\omega'' - k''V_0} \nabla^2 G_{k'',\omega''}(1,x') \right)$$

$$\cdot \left[\left\langle \phi_{k',\omega'}(1)\rho^*_{k',\omega'}(x') \right\rangle \left\langle \frac{d\phi_{k,\omega}(x')}{dx'} \frac{d\rho^*_{k,\omega}(2)}{dx_2} \right\rangle \right.$$

$$\left. - \left\langle \phi_{k',\omega'}(1)\phi^*_{k',\omega'}(x') \right\rangle \left\langle \frac{d\rho_{k,\omega}(x')}{dx'} \frac{d\rho^*_{k,\omega}(2)}{dx_2} \right\rangle \right] - \left(\frac{i}{\omega - kV_0} \nabla^2 G^*_{k,\omega}(2,x') \right)$$

$$\cdot \left[\left\langle \phi_{k',\omega'}(1)\rho^*_{k',\omega'}(x') \right\rangle \left\langle \frac{d\phi^*_{k'',\omega''}(x')}{dx'} \frac{d\rho_{k'',\omega''}(1)}{dx_1} \right\rangle \right.$$

$$\left. \left. - \left\langle \phi_{k',\omega'}(1)\phi^*_{k',\omega'}(x') \right\rangle \left\langle \frac{d\rho^*_{k'',\omega''}(x')}{dx'} \frac{d\rho_{k'',\omega''}(1)}{dx_1} \right\rangle \right] \right\},$$

and

$$B_3 = \sum_{\substack{k',\omega' \\ k,\omega}} \int dx' \left(\frac{i}{\omega'' - k''V_0} G_{k'',\omega''}(1,x') \right)$$

$$\cdot \left\{ k^2 \left\langle \frac{d\rho_{k',\omega'}(1)}{dx_1} \frac{d\phi^*_{k',\omega'}(x')}{dx'} \right\rangle \left\langle \rho_{k,\omega}(x')\rho^*_{k,\omega}(2) \right\rangle \right.$$

$$- \left\langle \frac{d\rho_{k',\omega'}(1)}{dx_1} \frac{d\rho_{k',\omega'}(x')}{dx'} \right\rangle \left\langle \phi_{k,\omega}(x')\rho^*_{k,\omega}(2) \right\rangle$$

$$- (k')^2 \left[\left\langle \rho_{k',\omega'}(1)\rho^*_{k',\omega'}(x') \right\rangle \left\langle \frac{d\phi_{k,\omega}(x')}{dx'} \frac{d\rho^*_{k,\omega}(2)}{dx_2} \right\rangle \right.$$

$$\left. \left. - \left\langle \rho_{k',\omega'}(1)\phi^*_{k',\omega'}(x) \right\rangle \left\langle \frac{d\rho_{k,\omega}(x')}{dx'} \frac{d\rho^*_{k,\omega}(2)}{dx_2} \right\rangle \right] \right\}.$$

To investigate vorticity correlation, we group terms containing some form of $\langle \rho\rho \rangle$ on the left of the equality. The rest of the triplet terms are placed on the right, and serve as a nonlinear source. Since we are most interested in small-scale structures, terms that are smooth functions of $\mathbf{x}_1 - \mathbf{x}_2$ shall be evaluated at $\mathbf{x}_1 = \mathbf{x}_2$. These "smooth" terms include those serving as a source, and those retained on the left of the equality with integral operators operated on. The integrated terms are smooth because the singularity of $\langle \delta\rho(1)\delta\rho(2) \rangle$ at $\mathbf{x}_1 = \mathbf{x}_2$ is logarithmic. After this arrangement, the "smooth" terms on the left cancel among themselves, and those on the right cancel up to terms that can be written as a total derivative in x. Hence, the remaining terms on the left appear as either $\langle \rho(1)\rho(2) \rangle$ or $\langle (d\rho(1)/dx_1)\,(d\rho(2)dx_2) \rangle$.

In other words, with the above operation it is seen that $[B_3]$ vanishes, that $(d/dx_1 + d/dx_2)\,[A(1,2)]$ becomes $d/dx_1\,[A(1,1)]$, a total derivative serving as a nonlinear source, and that $[B_1] + [B_2]$ becomes

$$\sum_{\substack{k',\omega' \\ k,\omega}} \left[k^2 \left(\frac{i}{\omega'' - k''V_0} \right) \left| \frac{d}{dx_1} \phi_{k',\omega'}(1) \right|^2 \left\langle \rho_{k,\omega}(1) \rho^*_{k,\omega}(2) \right\rangle \right.$$

$$-(k'')^2 \left(\frac{i}{\omega - kV_0} \right) \left\langle \frac{d\phi_{k',\omega'}(1)}{dx_1} \frac{d\phi^*_{k',\omega'}(2)}{dx_2} \right\rangle \cdot \left\langle \rho^*_{k'',\omega''}(1) \rho_{k'',\omega''}(2) \right\rangle \tag{A5}$$

$$+(k')^2 \left(\frac{i}{\omega'' - k''V_0} \right) \left\langle |\phi_{k',\omega'}(1)|^2 \right\rangle \cdot \left\langle \frac{d\rho_{k,\omega}(1)}{dx_1} \frac{d\rho^*_{k,\omega}(2)}{dx_2} \right\rangle$$

$$\left. -(k')^2 \left(\frac{i}{\omega - kV_0} \right) \left\langle \phi_{k',\omega'}(1) \phi^*_{k',\omega'}(2) \right\rangle \cdot \left\langle \frac{d\rho^*_{k'',\omega''}(1)}{dx_1} \frac{d\rho_{k'',\omega''}(2)}{dx_2} \right\rangle \right] \cdot e^{-iky_-}.$$

Now, we express $\left\langle (d\rho(1)/dx_1)\,(d\rho(2)/dx_2) \right\rangle$ as $-d^2/dx_-^2\,\langle \rho(1)\rho(2) \rangle$, and change the dummy index k'' to k, by which procedure a factor $e^{ik'y_-}$ will be introduced and attached to the coefficients $\left\langle d\phi(1)/dx_1 d\phi(2)/dx_2 \right\rangle$ and $\langle \phi(1)\phi(2) \rangle$. Finally, expanding these two coefficients at $\mathbf{x}_1 = \mathbf{x}_2$, $[B_1] + [B_2]$ can be expressed explicitly

$$\left[\left(D_{xx} k_0^2 y_-^2 + D_{yy} k_0^2 x_-^2 \right) \frac{\partial^2}{\partial x_-^2} + \left(D_{yy} k_0^2 y_-^2 + D''_y x_-^2 \right) \frac{\partial^2}{\partial y_-^2} \right] \langle \rho(1)\rho(2) \rangle \,,$$

where

$$\begin{bmatrix} D_{xx} \\ D_{yy} \\ D''_y \end{bmatrix} = \frac{1}{2\pi} \sum_{\substack{k' \\ \omega'}} \frac{i}{\omega' - k'V_0} \begin{bmatrix} (k')^2 \left\langle \phi^2 \right\rangle_{k',\omega'} \\ \left\langle (d\phi/dx)^2 \right\rangle_{k',\omega'} \\ \left\langle \left(d^2\phi/dx^2 \right)^2 \right\rangle_{k',\omega'} \end{bmatrix} \tag{A6}$$

and k_0 is the energy spectrum-averaged wavenumber. In the above expressions, a Markovian approximation has been used, where $i/(\omega'' - k''V_0)$ is replaced by $i/(\omega' - k'V_0)$. The approximation actually assumes the local resonance, $\omega - kV_0 = 0$.

This result has the following meaning. Turbulent convection tends to tear vorticity granulations apart. At small separation, vortex elements are convected by approximately the same turbulent velocity field, so that they experience less relative diffusion. Simultaneously, due to the spatial inhomogeneity, nonlinear effects locally redistribute the linear

source (due to the form of a total derivative w.r.t. x), thus yield a nonlinearly modified source.

When the turbulence level is not too large, as assumed throughout this work, the nonlinear source, $dA(1,1)/dx$, plays a less important role than the linear one and can thus be ignored.

References

1. Taylor, G. I. Phil., Trans. Roy. Soc. **A215**, 1 (1916).
2. Monin, A. S. and A. M. Yaglom, **Statistical Fluid Mechanics (I)**, Cambridge, MIT Press (1971).
3. Karman, T. von, Proc. Intern. Congr. Appl. Mech., Cambridge (1934).
4. Kolmogorov, A. N., J. Fluid Mech. **13**, 82 (1962); and C. R. Acad. Sci. URSS **30**, 301, 538.
5. Obukhov, A. M., J. Fluid Mech. **13**, 77 (1962).
6. Novikov, E. A., Sov. Phys. Dokl. **14**, 104 (1969).
7. Nelkin, M., Phys. Rev. **A9**, 388 (1974).
8. Mandelbrot, B., Lect. Note Math. **565**, 121 (1976).
9. Frisch, U., P.-L. Sulem, and M. Nelkin, J. Fluid Mech. **87**, 719 (1978).
10. Mori, H., Prog. Theor. Phys. **63**, 1044 (1980).
11. Kraichnan, R. H., J. Fluid Mech. **47**, 525 (1971).
12. Townsend, A. A., **The Structure of Turbulent Shear Flow**, Cambridge, Cambridge Press (1976).
13. Drazin, P. G. and W. H. Reid, **Hydrodynamical Stability**, Cambridge, Cambridge Press (1981).
14. Sagdeev, R. Z. and A. A. Galeev, **Nonlinear Plasma Theory**, Massachusetts, Benjamin Reading (1969).
15. Aref, H. and N. Pomphery, Phys. Lett. **78A**, 297 (1980).
16. Novikov, E. A. and Y. B. Sedov, Sov. Phys. JETP **50** (2) 297 (1980).
17. Haken, H., **Advanced Synergetic**, Berlin, Springer-Verlag (1983).
18. Benny, D. J. and R. F. Bergeron, Jr., Studies in Applied Math. **48**, 181 (1969).
19. Warn, T. and H. Warn, Studies in Applied Math. **59**, 37 (1978).
20. Christiansen, J. P. and N. J. Zabusky, J. Fluid Mech. **61**, 219 (1973).
21. McWilliams, J. C., J. Phys. Oceanogr. **11**, 921 (1984).
22. Brown, G. L. and A. Roshko, J. Fluid Mech. **64**, 775 (1974).
23. Dupree, T. H., Phys. Fluids (1974).
24. Sato, H. and K. Kuriki, J. Fluid Mech. **11**, 21 (1961).

25. Chiueh, T., P. W. Terry, P. H. Diamond, and J. E. Sedlak, Phys. Fluids **29**, 231 (1986).
26. Hasegawa, A. and M. K. Mima, Phys. Fluids **12**, 87 (1978).
27. Gill, A. E., **Atmosphere-Ocean Dynamics**, New York, Academic Press (1982).
28. Pringle, J. E., Ann. Rev. Astron. Astrophys. **19**, 137 (1981).
29. Nelson, D. R. in **Fundamental Problems in Statistical Mechanics (V)**, ed. by E. G. D. Cohen, North Holland (1980).
30. Dupree, T. H., Phys. Fluids **15**, 334 (1972).
31. Diamond, P. H., R. D. Hazeltine, Z. G. An, B. A. Carreras, and H. R. Hicks, Phys. Fluids **27**, 1449 (1984).
32. Leslie, D. C., **Developments in the Theory of Turbulence**, Oxford, Clarendon Press (1973).
33. Boustros-Ghali, T. and T. H. Dupree, Phys. Fluids **24**, 1839 (1981).
34. Batchelor, G. K., J. Fluid Mech. **5**, 113 (1959).
35. Terry, P. W. and P. H. Diamond, Phys. Fluids **28**, 1419 (1985).
36. Zabusky, N. J. and G. S. Deem, J. Fluid Mech. **47**, 353 (1971).
37. Aref, H. and E. D. Siggia, J. Fluid Mech. **109**, 435 (1981).
38. Everitt, K. W. and A. G. Robins, J. Fluid Mech. **88**, 563 (1978).
39. Shakura, N. I. and R. A. Sunyaev, Astron. Astrophys. **24**, 337 (1973).

Figure Captions

Fig. 1 A typical anisotropic equi-p contour of the vorticity spectrum, where $k_x > k_y$ due to mean flow shear.

Fig. 2 Vorticity $\mathbf{k}$-spectrum. At the low-$\mathbf{k}$ regime, the spectrum is anisotropic and obeys the power law p^{-2}; at the higher-$\mathbf{k}$ regime, the spectrum tends to become isotropic and a correction of $(\log)^{-n}$ to the $\mathbf{k}^{-2}$ power law is needed, where $n \leq 1/3$. At the largest scale of the wave regime, a spectral bump occurs due to the contribution from collective resonances.

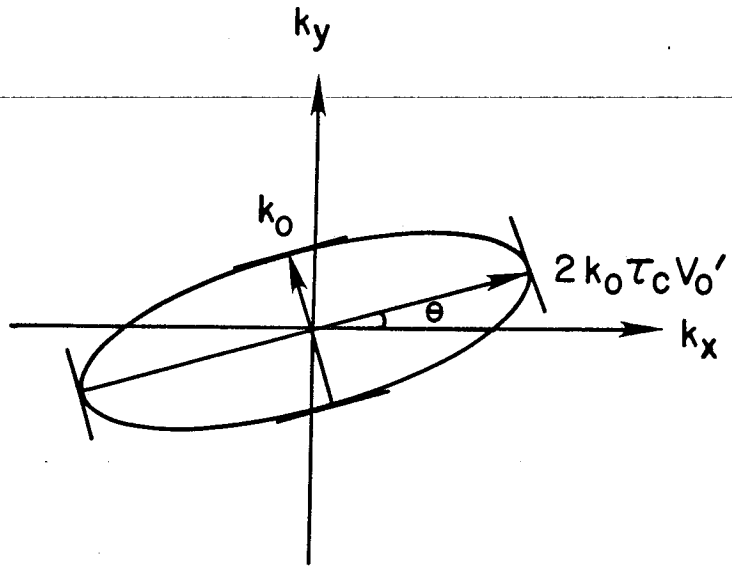

FIG. 1

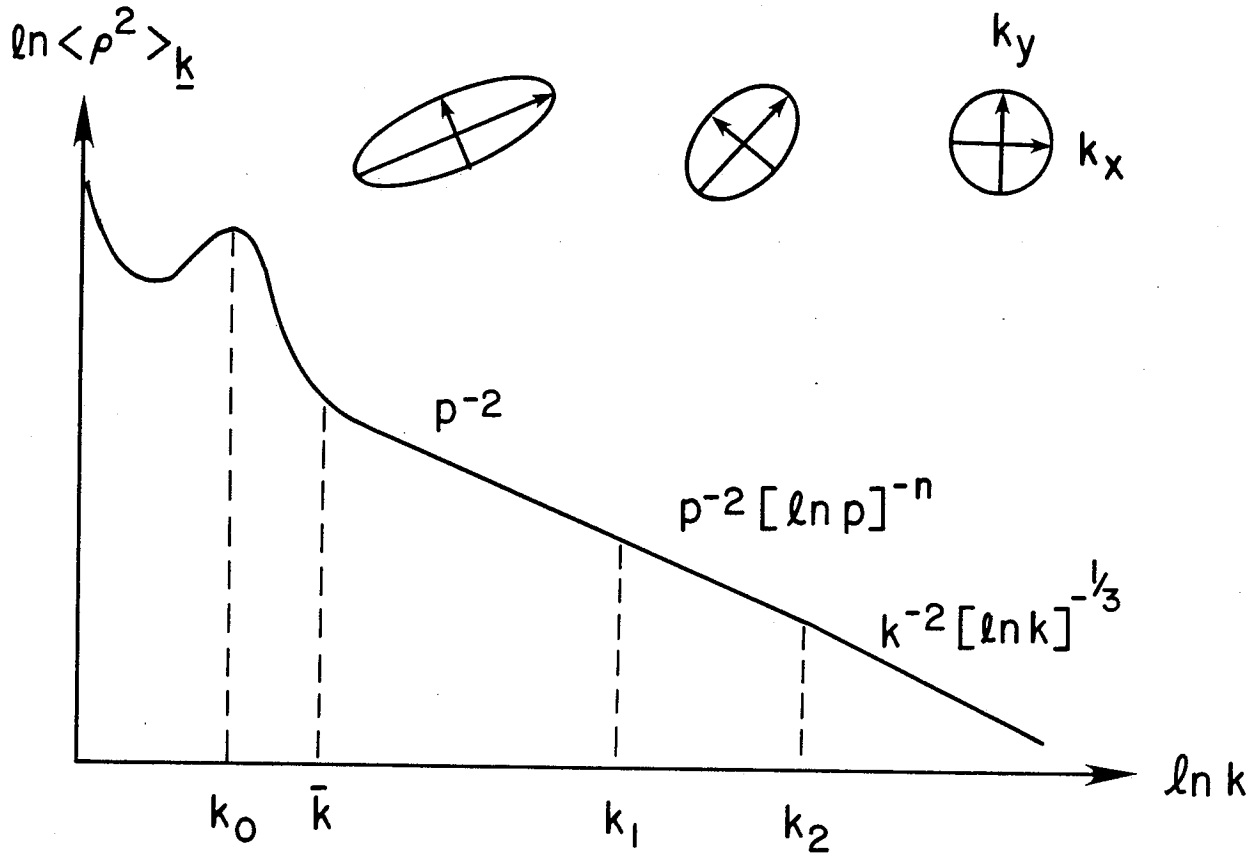

FIG. 2